Front. Electr. Electron. Eng. China 2007, 2(3): 355–360
DOI 10.1007/s11460-007-0067-y

RESEARCH ARTICLE

ZHANG Hanlei, ZHOU Jiemin, LI Gang

Improved wavelet analysis for induction motors mixed-fault diagnosis

Abstract Eccentricity is one of the frequent faults of induction motors, and it may cause rub between the rotor and the stator. Early detection of significant rub from pure eccentricity can prolong the lifespan of induction motors. This paper is devoted to such mixed-fault diagnosis: eccentricity plus rub fault. The continuous wavelet transform (CWT) is employed to analyze vibration signals obtained from the motor body. An improved continuous wavelet transform was proposed to alleviate the frequency aliasing. Experimental results show that the proposed method can effectively distinguish two types of faults, single-fault of eccentricity and mixed-fault of eccentricity plus rub.

Keywords induction motor, eccentricity, rub fault, mixed-fault, CWT, frequency aliasing

1 Introduction

Induction motors possess advanced features, such as simple construction, small volume, and light weight, which lead to their wide use in engineering applications. However, faults may occur after a long period of usage. Eccentricity is one of the frequent faults of induction motors [1], and the bearing abrasion may result in rotor eccentricity [2,3]. The bearing will be worn out during the usage, and the eccentricity will deteriorate. Radial force caused by eccentricity will bring about rub faults [4]. The abrasion caused by rub faults will make an induction motor fail to work in a fairly short time. Generally, there will be more than two kinds of faults existing in one motor. Moreover, certain faults incur others. So it is important to engage in the research of the mixed-fault diagnosis of induction motors. Meanwhile, it is necessary to detect rub faults as soon as possible.

Translated from *Proceedings of the Chinese Society for Electrical Engineering*, 2006, 26(8): 159–162 [译自: 中国电机工程学报]

ZHANG Hanlei (✉), ZHOU Jiemin, LI Gang
College of Aerospace Engineering, Nanjing University of Aeronautics and Astronautics, Nanjing 210016, China
E-mail: zhanghanlei@nuaa.edu.cn

Nowadays, there are lots of researchers engaging in the application of wavelet analysis in the field of fault diagnosis for induction motors. These mainly focus on single-faults, such as broken rotor bars [5,6], eccentricity [7,8], rotor-and-stator rub [9,10], etc. However, there are few reports on the wavelet-based mixed-fault diagnosis for troubles caused by the frequency aliasing in traditional wavelet transform. An improved wavelet analysis is developed here to detect the mixed-fault of the coexistence of eccentricity and rub.

Frequency aliasing of traditional wavelet transform can result in the overlapping of extracted signals, and finally lead to misdiagnosis. Through adjusting the peaks of Morlet wavelet in time scope, the frequency aliasing of wavelet transform will be efficiently eliminated, thus resulting in the reliability of the mixed-fault diagnosis for induction motors.

2 Continuous wavelet transform and band-pass filtering

If a compact-supported function $\psi(t)$ in $L^2(R)$ satisfies the admissible function condition [11]

$$C_\psi = \int_{-\infty}^{+\infty} \frac{|\Psi(\omega)|^2}{|\omega|^2} \mathrm{d}\omega < \infty \tag{1}$$

where

$$\Psi(\omega) = \int_{-\infty}^{\infty} \psi(t) \mathrm{e}^{-\mathrm{j}\omega t} \mathrm{d}t \tag{2}$$

it can be used as an analytical function in the continuous wavelet transform. For a finite energy function $f(t)$, its continuous wavelet transform [12] is defined as

$$W_\psi f(a,b) = \frac{1}{\sqrt{a}} \int_{-\infty}^{\infty} f(t) \bar{\psi}\left(\frac{t-b}{a}\right) \mathrm{d}t \tag{3}$$

where $a>0$ is called the scale factor, b is the time-shift, and $\bar{\psi}(t)$ denotes the complex conjugation of $\psi(t)$.

Furthermore, by changing the original wavelet function into

$$g_a(t) = \frac{1}{\sqrt{a}} \bar{\psi}(-t) \tag{4}$$

the wavelet transform in Eq. (3) can be written as a filtering operation

$$W_g f(a,b) = \int_{-\infty}^{\infty} f(t) g\left(\frac{b-t}{a}\right) \mathrm{d}t = f(t) * g_a(t) \tag{5}$$

where $*$ denotes the convolution.

When the amplitude-frequency characteristic of $\hat{\psi}(\omega)$ is concentrative, the continuous wavelet transform of a signal using continuous wavelets of different scale factors seems as if the signal is put through a bunch of band-pass filters [13]. Scale factors determine the bandwidth and central frequency of the band-pass filter. Hence, after choosing factors appropriately, we can use continuous wavelet transform to extract certain frequency components of a signal.

3 Improved Morlet wavelet analysis

In this paper, Morlet wavelet function is employed as the base function of the wavelet transform. The Morlet wavelet is defines as

$$\psi(t) = \mathrm{e}^{\mathrm{j}\omega_0 t - t^2/T} \tag{6}$$

Morlet wavelet is a single-frequency sine function enveloped by a Gaussian function [14].

Here is the Morlet wavelet in frequency domain

$$\psi(t) = \sqrt{\frac{\pi}{T}} \mathrm{e}^{T(\omega-\omega_0)^2/4} \tag{7}$$

The central frequency of Morlet wavelet $\psi(t)$ is ω_0, and its bandwidth is $2\sqrt{1/T}$. After the operation of expanding, contracting and translating, the central frequency of Morlet wavelet $\psi_{a,b}(t)$ will be ω_0/a, and its bandwidth $2\sqrt{1/T}/a$.

The real part of Morlet wavelet is employed as the base wavelet function. The following is the real part of the traditional Morlet wavelet function [15]

$$\psi(t) = \mathrm{e}^{-\frac{t^2}{2}} \cos 6t \tag{8}$$

Equation (9) is the analytical Morlet wavelet function, which is the adjusted result from the base function by the scale factor a

$$\psi_a(t) = \mathrm{e}^{-t^2/(2a^2)} \cos\frac{6t}{a} \tag{9}$$

After normalized computation, when a equates $1/40\pi$, the central frequency of $\psi_a(t)$ is 100 Hz. Figure 1(a) is the time domain waveform of $\psi_a(t)$, and Fig. 1(b) is the spectrum of $\psi_a(t)$. The window of the spectrum in Fig. 1(b) totally overlaps the 75 Hz frequency, which subsequently leads to troubles that the extracted signal of 100 Hz central frequency contains 75 Hz frequency component.

In the process above, there are three obvious peaks in the traditional Morlet wavelet function. To narrow down the window of the spectrum, one can increase the number of peaks in the time domain waveform of the base function. Figure 2(a) is the time domain waveform of Morlet wavelet whose peak number is five, and Fig. 2(b) is its spectrum. After comparison, one can find that the bandwidth of the adjusted base function is narrower than that of the original one. In this way, the result of the wavelet transform could be greatly improved.

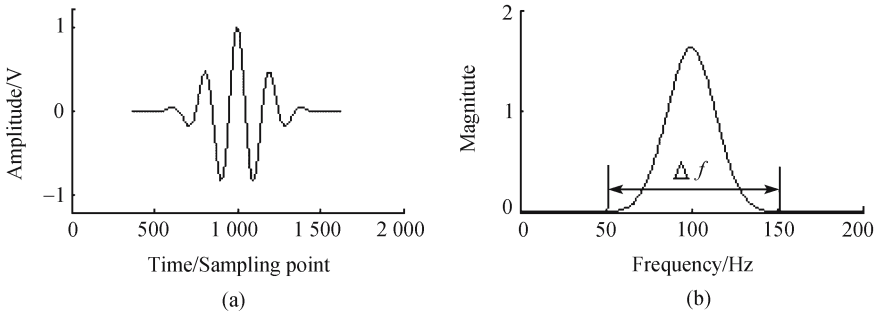

Fig. 1 Morlet wavelet of three peaks and its spectrum

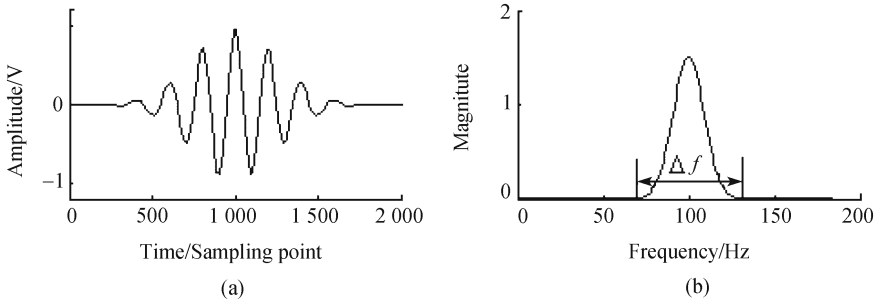

Fig. 2 Morlet wavelet of five peaks and its spectrum

4 Experimental results

A three-phase induction motor is employed to demonstrate the discussed method. Specifications of the experimental motor are shown in Table 1.

Table 1 Specifications of the experimental rotor

Ratings	Magnitude
Rated power	40 W
Rated voltage	380 V
Rated current	0.24 A
Rated speed	2 800 r·m^{-1}

Three types of faults, eccentricity, mixed-fault of eccentricity plus mild rub fault, and mixed-fault of eccentricity plus moderate rub fault are set on the induction motor. Vibration signals on the motor body are the analyzed signals, which are acquired using the test system in Fig. 3. An acceleration meter is used to transform vibration signals into voltage signals; a charge amplifier is used to gain higher signal-to-noise ratio. A multifunctional digital oscilloscope is employed to capture and store signals; finally, the data are stored in a computer and processed by continuous wavelet transform.

Figure 4 shows the vibration signals acquired from the body of the induction motor in field application. Each signal

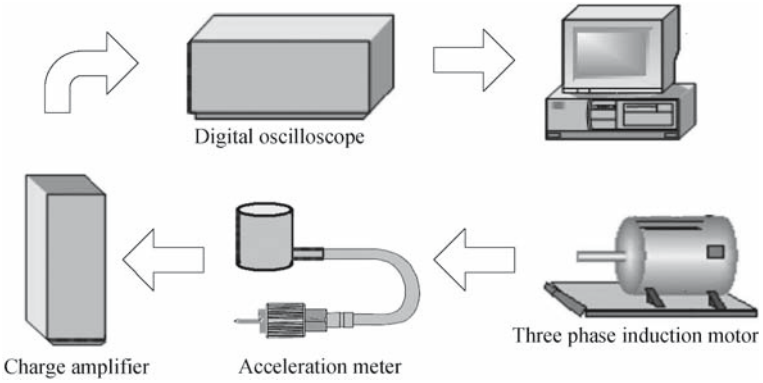

Fig. 3 Vibration signal testing system

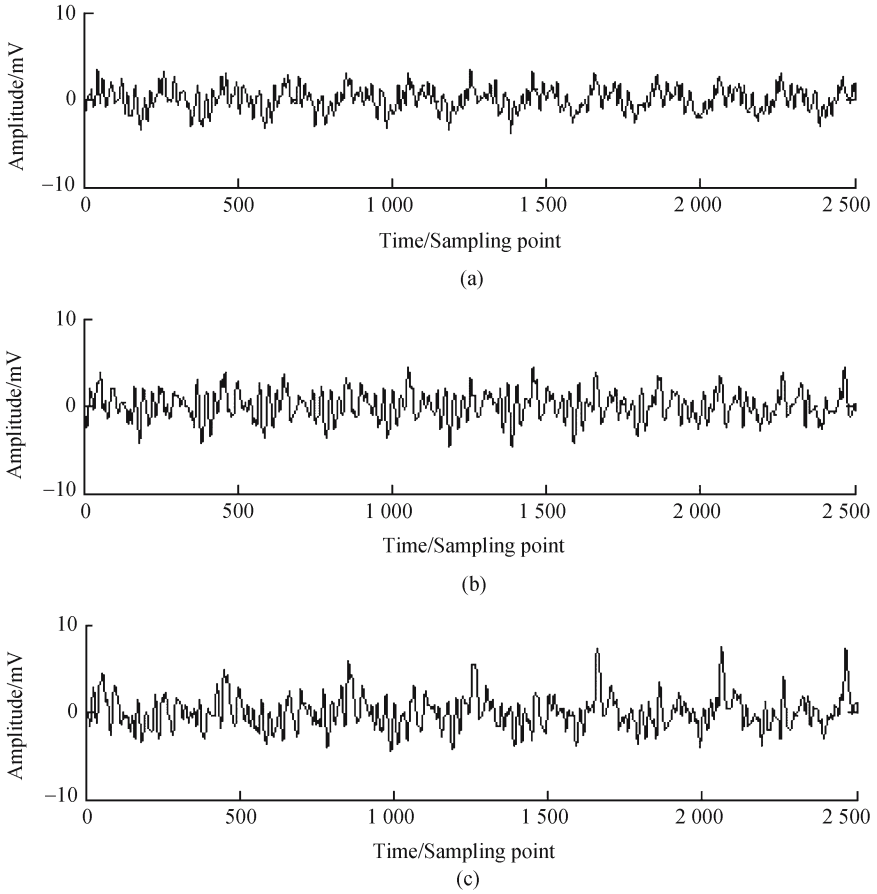

Fig. 4 Vibration signals of (a) eccentricity; (b) mixed-fault of eccentricity plus mild rub; (c) mixed-fault of eccentricity plus moderate rub

has multi-frequency and is noisy. It is difficult to distinguish the difference between these signals with naked eyes.

4.1 Traditional CWT result

The vibration signals are processed by continuous wavelet transform using the traditional Morlet base function with three peaks. The central frequencies of the continuous wavelet transform are set as 25, 75, and 100 Hz respectively. The wavelet transform can be written as a filtering operation, so the result of the continuous wavelet transform can be regarded as extracted sub-band frequency signals. The results of traditional continuous wavelet transform are shown in Fig. 5. The 25 Hz sub-band frequency signals are similar to a pure sine function, which illuminates that there is only one frequency component. According to the fault theory of induction motors, the extracted 25 Hz sub-band frequency signal is reasonable. However, the 75 and 100 Hz sub-band frequency signals are mixed. Checking the spectrums of the sub-band frequency signals, one can discover the overlapping results from the frequency aliasing. This kind of overlapping may bring about misdiagnosis. Frequency aliasing must be eliminated for a reliable diagnosis.

4.2 Improved CWT result

To solve the frequency aliasing problem, an improved Morlet base function is proposed here. As shown in Figs. 1 and 2, after increasing the peaks of Morlet wavelet in time domain, the bandwidth of the Morlet wavelet can be narrowed down significantly. Thus, it can be deduced that the result of continuous wavelet transform using five-peak Morlet wavelet can alleviate the frequency aliasing.

The results of the improved continuous wavelet transform of the vibration signals are shown in Fig. 6. The 25 Hz sub-band frequency signals in Figs. 5 and 6 are coincident. The overlapping of the 75 and 100 Hz sub-band frequency signals are alleviated remarkably. Checking the spectrums of the sub-band frequency signals, one can find that each of the extracted results has only one frequency component. The extraction of sub-band frequency signals is efficient. Therefore, we can draw the conclusion that increasing the peaks of Morlet

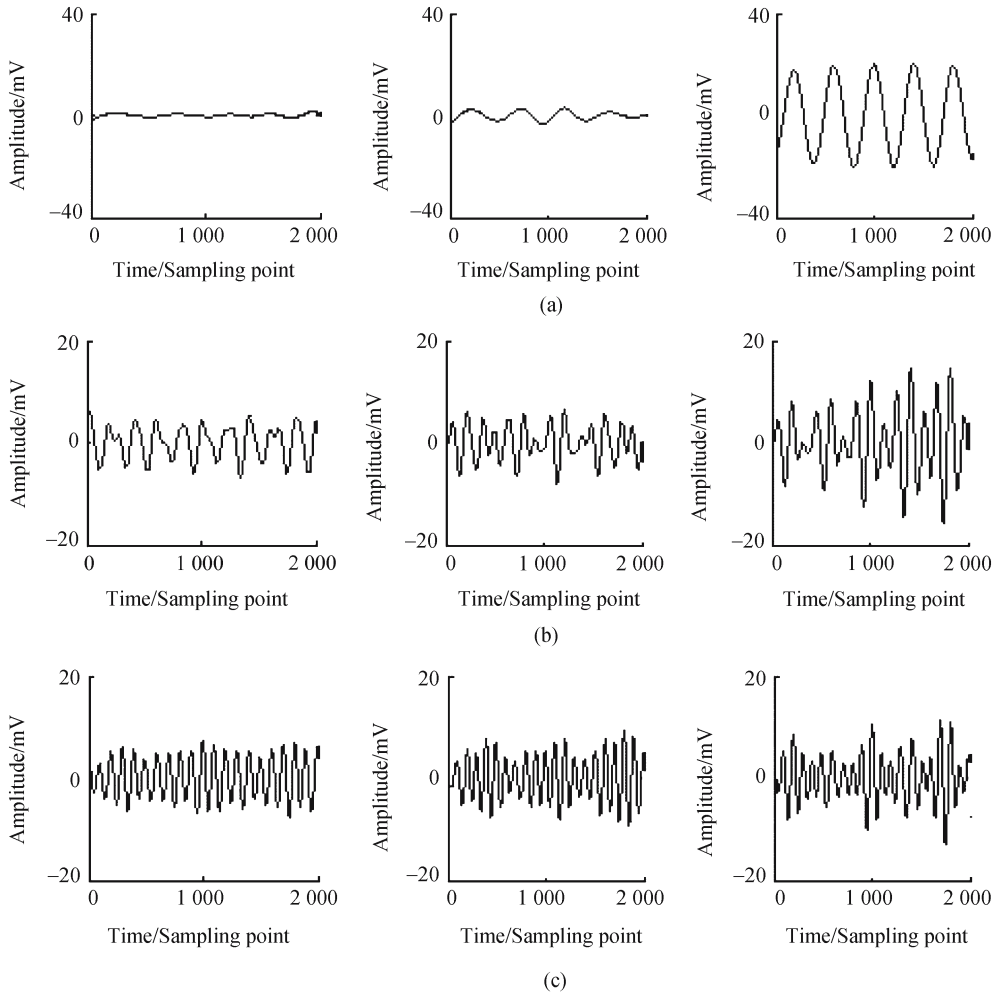

Fig. 5 Sub-band frequency signals of: (a) 25; (b) 75; (c) 100 Hz extracted using three-peak Morlet wavelet

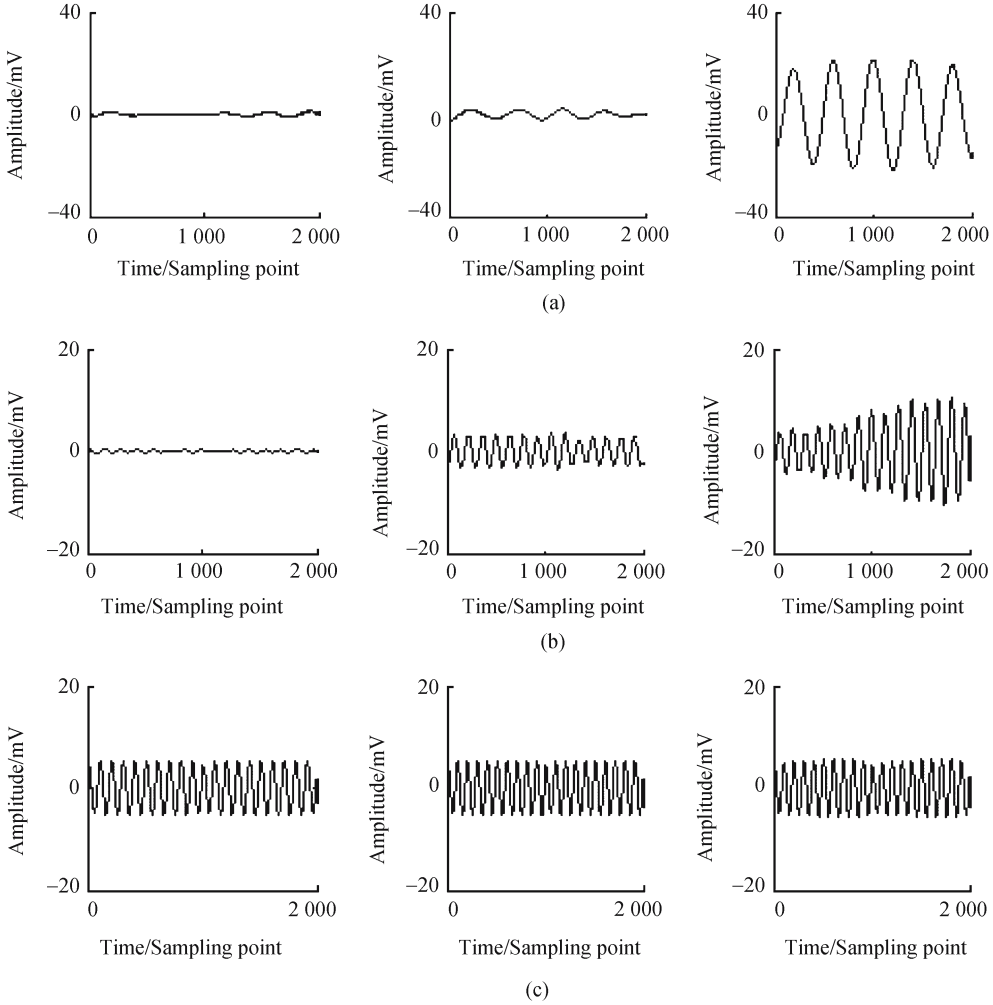

Fig. 6 Sub-band frequency signals of: (a) 25; (b) 75; (c) 100 Hz extracted using five-peak Morlet wavelet

wavelet can release the frequency aliasing of continuous wavelet transform effectively. The extracted results are more reliable than using the traditional continuous wavelet transform.

In addition, in Fig. 6 the 100 Hz sub-band frequency signals of different faults have no obvious difference. A conclusion can be drawn that the occurrence of the rub fault has no effect in this frequency range.

4.3 Contrasts

The energy equation shown in Eq. (10) is employed here to evaluate the proposed method [6]

$$E_i = E[w_i^2(t)] = \frac{1}{T}\int_0^T w_i^2(t)\mathrm{d}t \tag{10}$$

Table 2 lists the energy value of the transformed sub-band frequency signals by the traditional continuous wavelet transform. One can find that the energy value of the 75 Hz sub-band frequency signals increases less than that of the 100 Hz sub-band frequency signals after mild rub fault occurs. The energy value of the 100 Hz sub-band frequency signals increases even more after moderate rub fault occurs. This result is not reasonable, and it will lead to misdiagnosis.

Table 2 Energy value of sub-band frequency signals extracted using three-peak Morlet wavelet

Faults	Frequency of extracted signals		
	25 Hz	75 Hz	100 Hz
Eccentricity	0.629	10.534	13.586
Eccentricity plus mild rub	3.714	10.851	14.029
Eccentricity plus moderate rub	172.25	33.434	16.093

Table 3 lists the energy value of the transformed sub-band frequency signals with the improved continuous wavelet transform. After the rub fault occurs, energy values of the 25 and 75 Hz sub-band frequency signals increase significantly, and energy values of the 100 Hz sub-band frequency signals change slightly. By taking the energy values of the 25 and 75 Hz sub-band frequency signals as fault eigenvalues, the two kinds of faults, single-fault of eccentricity and mixed-fault of eccentricity plus rub, can be distinguished effectively.

Table 3 Energy value of sub-band frequency signals extracted using five-peak Morlet wavelet

Faults	Frequency of extracted signals		
	25 Hz	75 Hz	100 Hz
Eccentricity	0.025	0.042	0.259
Eccentricity plus mild rub	0.124	0.126	0.258
Eccentricity plus moderate rub	11.859	0.642	0.259

5 Conclusions

In this paper, an improved wavelet transform method is proposed to analyze vibration signals for induction motor diagnosis. With continuous wavelet transform, certain frequency components are extracted from vibration signals. This method can clearly exhibit the time-frequency characteristic of fault signals. By increasing the peaks of the time domain waveform of analysis function, misdiagnosis caused by frequency aliasing can be effectively eliminated. The proposed method provides a promising way for the mixed-faults diagnosis of induction motors.

References

1. Liu Zhenxing, Yin Xianggen, Zhang Zhe. Online rotor-mixed fault diagnosis way based on spectrum analysis of instantaneous power in squirrel cage induction motors. IEEE Trans Energy Conversion, 2004, 19(3): 485–490
2. Zhou Feng, Wang Mingyu, Du Yanwei. Summary of online monitoring and fault diagnosis technique for induction motor based on MCSA. Journal of Chongqing University (Natural Science Edition), 2005, 28(1): 49–52 (in Chinese)
3. Liu Zhengxing, Zhang Zhe, Yin Xianggen. A summary of online condition monitoring and fault diagnostics for 3-phase induction motors. Journal of Wuhan University of Science and Technology (Natural Science Edition), 2001, 24(3): 285–289 (in Chinese)
4. Xiang Ling, Hu Aijun, Tang Guiji. Study of emulation and test on fault of rotor-to-stator rub-impact. Lubrication Engineering, 2005, 5: 78–80 (in Chinese)
5. Douglas H, Pillay P, Ziarani A K. Broken rotor bar detection in induction machines with transient operating speeds. Energy Conversion of IEEE Transactions, 2005, 20(1): 135–141
6. Cao Zhitong, He Guoguang, Chen Hongping. Multiple bandwidth wavelet analysis for fault diagnosis eigenvalue in squirrel-cage induction motor. Proceedings of the CSEE, 2003, 23(7): 112–116 (in Chinese)
7. Hamidi H, Nasiri A R, Nasiri F. Detection and isolation of mixed eccentricity in three phase induction motor via wavelet packet decomposition. The 5th Asian Control Conference, 2004, 2: 1 371–1 376
8. Nasiri A, Poshtan J, Kuhaei M H. Wavelet packet decomposition as a proper method for fault detection in three phase induction motor. IEEE International Conference on Mechatronics, 2004, 1: 13–18
9. Hu Niaoqing, Wen Xisen. Analysis and identification methods for vibration characteristics of rotor rub-impact fault. Proceedings of the CSEE, 2002, 22(12): 70–73 (in Chinese)
10. Li Ruixin, Wang Dongfeng, Han Pu. On the applications of SVD in fault diagnosis. IEEE International Conference on Systems, Man and Cybernetics, 2003, 4(5): 3763–3768
11. Peng Zhike, He Yongyong, Lu Qing. Using wavelet method to analyze fault features of rub rotor in generator. Proceedings of the CSEE, 2003, 23(5): 75–79 (in Chinese)
12. Li Xianxiang, Xu Xiaozeng, Xiao Hongjun. The speed-adjustment system of brush DC motor based on wavelet ann. Proceedings of the CSEE, 2005, 25(9): 126–129 (in Chinese)
13. Zhang Xiaofen, Li Gongyan. Extraction of fault diagnosis signal's frequency band with wavelet analysis. Journal of Vibration and Shock, 2004, 23(4): 47–50 (in Chinese)
14. Jiang Dongxiang, Diao Jinhui, Zhao Gang. Study on methods of vibration fault diagnosis based on time-frequency contour map for turbine generator unit. Proceedings of the CSEE, 2005, 25(6): 146–151 (in Chinese)
15. Xue Hui, Yang Rengang. Morlet wavelet based detection of non-integer harmonics. Power System Technology, 2002, 26(12): 41–44 (in Chinese)